

1 **High energy supercapattery with an ionic liquid solution of LiClO<sub>4</sub>**

2 Linpo Yu,<sup>a,b</sup> and George Z. Chen<sup>a,b\*</sup>

3 <sup>a</sup> *Department of Chemical and Environmental Engineering, and Energy and Sustainability*

4 *Research Division, the University of Nottingham, Nottingham, NG7 2RD UK*

5 *Email: [George.Chen@nottingham.ac.uk](mailto:George.Chen@nottingham.ac.uk)*

6 <sup>b</sup> *Department of Chemical and Environmental Engineering, and Centre for Sustainable Energy*

7 *Technologies, Faculty of Science and Engineering, the University of Nottingham Ningbo China,*

8 *Ningbo, 315100 China*

9

10 **Abstract:**

11 Supercapattery combining an ideally polarized capacitor-like electrode and a battery-like  
12 electrode is demonstrated theoretically and practically using an ionic liquid electrolyte  
13 containing 1-butyl-1-methylpyrrolidinium tri(pentafluoroethyl)trifluorophosphate (BMPyrFAP),  
14 gamma-butyrolactone ( $\gamma$ -GBL) and LiClO<sub>4</sub>. The electrochemical deposition and dissolution of  
15 lithium metal on a platinum and glass carbon electrode were investigated in this ionic liquid  
16 solution. The CV data shows the fresh electrochemical deposited lithium metal is stable in the  
17 electrolyte, which encourages the investigation of this ionic liquid solution in supercapattery  
18 with a lithium battery negative electrode. The active material counted specific energy of the  
19 supercapattery based on a lithium negative electrode and an activated carbon (Act-C) positive  
20 electrode can reach 230 Wh kg<sup>-1</sup> under the Galvanostatic charge-discharge current density of 1  
21 mA cm<sup>-2</sup>. The positive electrode material, Act-C was also investigated by CV, AC impedance,  
22 SEM and BET. The non-uniform particle size and micropore porous structure of the Act-C  
23 enable its electric double layer capacitor (EDLC) behavior in the ionic liquid solution. The

1 calculated specific capacitance of the Act-C in this ionic liquid solution is higher than same Act-  
2 C in aqueous solution, which indicates the pseudocapacitance behaviour of Act-C with the  
3 species in the ionic liquid electrolyte.

4

## 5 **Introduction**

6 Supercapattery (=supercapacitor + battery) takes the advantages of both supercapacitor  
7 (also known as electric double layer capacitor, or EDLC) and battery by combining an ideally  
8 polarized capacitor-like electrode and a battery-like electrode.<sup>1</sup> Although lithium ion capacitor<sup>2,3</sup>  
9 is also comprised of this hybrid configuration, supercapattery is the more general term of the  
10 particular design.

11 In theory, supercapattery can possess higher energy density than both battery and  
12 supercapacitor and can supply this energy at a power output almost as high as supercapacitor.  
13 The high power output of supercapattery is mainly a result of sharing the same electrochemical  
14 active materials with supercapacitor, where the nanostructured carbons, like activated carbon  
15 (Act-C), carbon nanotubes (CNTs) and graphene are the best choice for the ideally polarized  
16 electrode because of their large surface area, porosity, stability over a wide potential window,  
17 and intrinsically low electrical resistance. In addition, pseudo-capacitive materials including  
18 MnO<sub>2</sub>, RuO<sub>2</sub> and conducting polymers can also be used as the capacitor-like electrode materials  
19 providing the high electrode capacitance, but limiting the potential windows.

20 As to the battery-like electrode, various electrode materials from commercial battery  
21 systems can be the candidate, from lead acid batteries to metal/air systems, but in practice, metal  
22 compounds<sup>3-5</sup> like SnO<sub>2</sub>, MnO<sub>2</sub> and LiFePO<sub>4</sub> are more common and commercially available.  
23 Theoretically, the hypothetical battery comprising lithium metal and fluorine gas (Li-F battery)

1 would output a cell voltage about 6.1 V and offer a specific energy content of 6304 Wh kg<sup>-1</sup>. Any  
2 battery cannot go beyond the specific energy content of the hypothetical Li-F battery. As to Li-  
3 ion battery (Li<sub>x</sub>C<sub>6</sub> | Li<sub>1-x</sub>CoO<sub>2</sub>), the theoretical specific energy is 552 Wh kg<sup>-1</sup> at 3.5 V. A  
4 hypothetical supercapattery comprising a lithium metal negative electrode and a supercapacitor  
5 positive electrode (assumed 400 F g<sup>-1</sup>) is evaluated and analyzed here. Considering the specific  
6 charge capacity of lithium is much larger than that of the supercapacitor electrode, the mass of  
7 the lithium metal is negligible. The theoretical specific energy value would be 625 Wh kg<sup>-1</sup> for  
8 the cell voltage vary from 3.5 V to 1.0 V. This theoretical value is even higher than the one of  
9 the Li-ion battery.

10 The above calculation is based on the equation of the capacitor energy, Eq. 1,

$$11 \quad E_{\max} = \frac{1}{2} C U_{\max}^2 \quad (1)$$

12 where  $C$  is the specific capacitance of a capacitor, and  $E_{\max}$  is the maximum energy capacity of a  
13 capacitor correlated to its maximum tolerable voltage,  $U_{\max}$ . It should be mentioned that a hybrid  
14 cell of a battery electrode and a supercapacitor electrode does not always show typical  
15 supercapacitor behaviour, where the cell voltage ( $U$ ) is always proportional to the time ( $t$ ) during  
16 a constant current charging or discharging test. If the cell presents battery like features, the term  
17 supercabattery is recommended,<sup>6</sup> but not discussed in this paper. In the case of supercapattery,  
18 the  $U_{\max}$  is a key factor for the energy capacity of the devices. Because the behaviour of  
19 supercapattery is close to that of supercapacitor,<sup>1</sup> several strategies that have been applied in  
20 supercapacitor can be utilized in supercapattery to improve the practical energy capacity, such as  
21 using the design of asymmetric supercapacitor cell,<sup>7</sup> controlling the capacitance ratio of the  
22 positive and negative electrode made from the same material,<sup>8</sup> and serially stacking the cells  
23 through the bipolar electrodes.<sup>9</sup> Apart from these efforts based on the aqueous electrolytes, there

1 is a strong desire for changing the aqueous to organic electrolytes to achieve a high working  
2 voltage.

3 Recent studies have revealed both aqueous and non-aqueous supercapatteries using lithium  
4 metal<sup>10</sup> and Li-ion battery material<sup>3</sup> as the electrode. An aqueous supercapattery consisting of a  
5 MnO<sub>2</sub> positive electrode and a Li/LISICON/PEO-LiTFSI/Li<sup>+</sup> negative electrode had achieved a  
6 specific energy capacity of 114 Wh kg<sup>-1</sup> with a 4.3 V cell voltage.<sup>10</sup> The Li/LISICON/PEO-  
7 LiTFSI/Li<sup>+</sup> electrode is a multi-layered Li electrode, which consists of lithium metal, a  
8 LISICON-type solid glass ceramic as the water-stable solid electrolyte, and a buffer layer  
9 consisting of polyethylene oxide with Li(CF<sub>3</sub>SO<sub>2</sub>)<sub>2</sub>N polymer electrolyte (PEO-LiTFSI) between  
10 the lithium metal and the solid electrolyte. If MnO<sub>2</sub> is replaced by RuO<sub>2</sub> as the positive electrode,  
11 the specific energy capacity of the device comes to 520 Wh kg<sup>-1</sup> with a 3.8 V cell voltage.<sup>10</sup>  
12 However, the current density of the aforementioned devices is only 0.255 mA cm<sup>-2</sup>, which is  
13 limited by the solid/liquid interphase. This disadvantage prevents these high energy capacity  
14 devices in any high power application. Another non-aqueous supercapattery using LiFePO<sub>4</sub> as  
15 the positive electrode and Cabot carbon black as the negative electrode possesses good cycling  
16 stability at high current density in a Li-ion contained propylene carbonate (PC) electrolyte.<sup>3</sup>  
17 However, the potential range of the Cabot carbon black can only keep its capacitor-like  
18 behaviour from 2.80 to 1.25 V vs. Li/Li<sup>+</sup> in the electrolyte, which has limited the cell voltage.

19 Ionic liquids are specially featured by their zero or negligible volatility, but still able to offer  
20 the highly ionic environment, and wide temperature and potential windows.<sup>11</sup> They have brought  
21 about unique opportunities, including synthesis,<sup>12</sup> trace analysis,<sup>13,14</sup> thermochromic/cryochromic  
22 materials,<sup>15-17</sup> and electrochemical energy storage.<sup>18-20</sup> Consequently, ionic liquid solutions can

1 be chosen as competitive candidates for the electrolytes of supercapattery when the battery-  
2 behaviour electrode is a lithium-ion or lithium battery negative electrode.

3 Here, we report the recent supercapattery work based on an activated carbon positive  
4 electrode and a Li/Li<sup>+</sup> negative electrode using an ionic liquid electrolyte, 1-butyl-1-  
5 methylpyrrolidinium tri(pentafluoroethyl)trifluorophosphate (BMPyrrFAP) containing gamma-  
6 butyrolactone ( $\gamma$ -GBL) and LiClO<sub>4</sub>. The characterization of the activated carbon has been done  
7 and presented here, including the data of cyclic voltammogram (CV), AC impedance, SEM and  
8 BET. The demonstrated supercapattery cell shows a clear capacitor-like behaviour in the CV and  
9 Galvanostatic charge and discharge (GCD) tests. This particular hybrid design ensures the full  
10 usage of the electrochemical window of the ionic liquid solution and the capacitance of the  
11 activated carbon, and basically maintains the high power of the supercapacitor.

12

### 13 **Experimental**

14 In this work, a supercapacitor grade commercial product of activated carbon (Act-C, YP50F,  
15 Kuraray Chemical Co.) was used. The other chemicals, 1-butyl-1-methylpyrrolidinium  
16 tri(pentafluoroethyl)trifluorophosphate (BMPyrrFAP, Merck), 1-ethyl-3-methylimidazolium  
17 tetracyanoborate (EMIM[B(CN)<sub>4</sub>], Merck), gamma-butyrolactone ( $\gamma$ -GBL, Sigma Aldrich) and  
18 LiClO<sub>4</sub> (Sigma Aldrich), were commercially available and used without further purification.  
19 Lithium metal (foil, Sigma Aldrich) was kept and handled in an argon filled glove box. The  
20 homemade electrochemical cells (2-electrode/3-electrode cells and sandwich type cell) were  
21 fabricated in an argon-filled glove box (O<sub>2</sub> < 10 ppm, H<sub>2</sub>O < 10 ppm) and transferred outside the  
22 glove box for the electrochemical experiments by an AUTOLAB 302N potentiostat. Membrane  
23 from Celgard was used as the separator in the sandwich type cell.

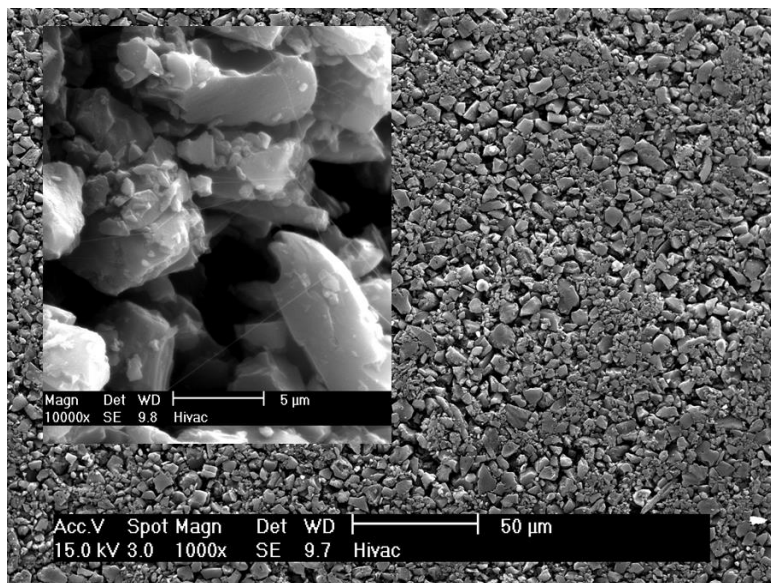
1 For the electrochemical tests, the Act-C powder was made into pellet type and casted  
2 electrodes with PTFE and PVDF, respectively. The details of fabricating the Act-C/PTFE pellet  
3 electrode can be found in previous publication from this laboratory.<sup>21</sup> The Act-C/PVDF electrode  
4 was fabricated by the following process. 10  $\mu\text{L}$  of an Act-C suspension (0.950 g Kuraray Act-C  
5 and 0.050 g PVDF powder in 20 mL DMSO suspension) was dropped on a 5 mm diameter  
6 graphite disc electrode. The electrode loaded with 0.5 mg of Act-C composite (95 % w. Act-C  
7 and 5 % w. PVDF) was dried in a vacuum oven at 75 °C overnight, and then was ready for the  
8 electrochemical tests.

9 All the experiment is operated at room temperature. More experimental details are specified  
10 in the following sections.

## 12 Results and discussion

13 The pore size and volume distribution of an Act-C are the most important physical  
14 characteristics. Fig. 1 presents the SEM images of an Act-C pellet containing 5 % w. PTFE. The  
15 Act-C powder is non-uniform in particle size, and the PTFE is binding the Act-C particles like a  
16 spider web to maintain the mechanical strength of the Act-C pellet. The surface area of the  
17 Kuraray Act-C sample is 1724  $\text{m}^2 \text{g}^{-1}$  determined from the nitrogen absorption/desorption  
18 isotherms at 77 K (ASAP 2420) by applying the density function theory (DFT). In previous  
19 work,<sup>21</sup> the dominant range of pore widths of the same Kuraray Act-C sample is between 1.5 and  
20 2.5 nm. For an aqueous electrolyte, its wetting ability with the Act-C pellet will affect the contact  
21 between the electrolyte and Act-C particles, and vary the charge storage performance of the Act-  
22 C sample. As to the organic electrolyte, the wetting is not a problem anymore, while the  
23 interaction between electrolyte and carbon materials inside the pore will play an important role.

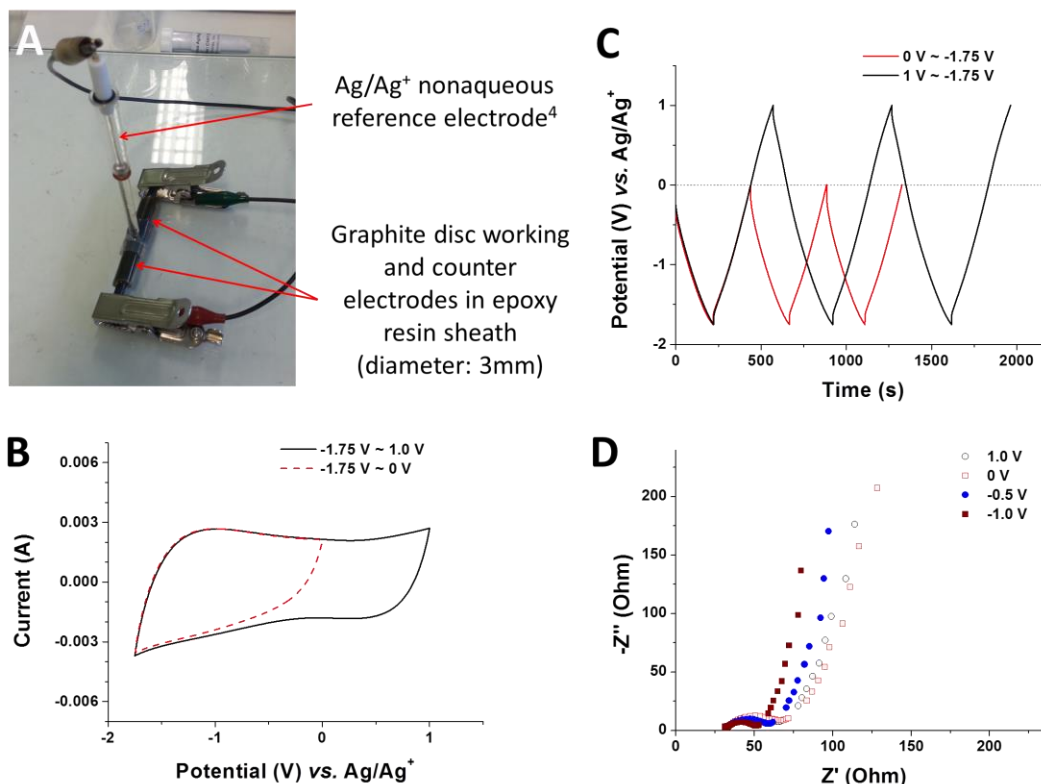
1 A theory was proposed for the traditional organic electrolyte, that the longer the pore inside the  
2 particle is, the poorer performance of the capacitance of the porous carbon materials is.<sup>3</sup> This is  
3 mainly due to the ion block of the pores by the non-ionic solvent molecular. Similar phenomenon  
4 was also observed in the case of aqueous electrolyte with organic additive.<sup>21</sup>



5  
6 **Fig. 1** SEM images of the activated carbon pellet (including 5 % w. PTFE). The insert is the  
7 enlarge view of the back image.

8  
9 Before the work on the supercapattery, we have investigated the Kuraray **Act-C** in a  
10 commercial ionic liquid, 1-ethyl-3-methylimidazolium tetracyanoborate (EMIM[B(CN)<sub>4</sub>]). Fig. 2  
11 shows the photo of electrochemical tube cell and test results on CV, GCD and AC impedance. A  
12 small piece of **Act-C** pellet (about 1 mg, containing 5 % w. PTFE) was loaded on a 6 mm  
13 diameter graphite disc electrode. Another graphite disc attaching 30 mg **Act-C** was used as the  
14 counter electrode. Reference electrode is a Ag/Ag<sup>+</sup> electrode filled with 0.01 mol L<sup>-1</sup> AgNO<sub>3</sub>  
15 acetonitrile solution, which is connected to the electrolyte via a salt bridge filled with  
16 EMIM[B(CN)<sub>4</sub>]. This reference can be prepared following the method described in reference.<sup>22</sup> It

1 should be mentioned that the reference electrode is **changed** to Li/Li<sup>+</sup> electrode in the latter  
2 discussion except in Fig. 2. Any potential in this paper will be suffixed with the reference  
3 electrode used in the experiment.



4  
5 **Fig. 2 (A):** Photograph of the tube cell. 1.064 mg **Act-C** (including 5% w. PTFE) was loaded on  
6 the graphite disc as working electrode. EMIM[B(CN)<sub>4</sub>] was filled in the tube as electrolyte.  
7 Reference electrode is Ag/Ag<sup>+</sup> electrode in 0.01 mol L<sup>-1</sup> AgNO<sub>3</sub> acetonitrile solution connected  
8 to the electrolyte via a salt bridge filled only with EMIM[B(CN)<sub>4</sub>]. The results in **(B)**, **(C)** and  
9 **(D)** were collected from this tube cell.

10 **(B):** CVs of the tube cell. Scan rate: 20 mV s<sup>-1</sup>.

11 **(C):** Galvanostatic Charge-Discharge plots of the tube cell. Current: 1 mA.

12 **(D):** Nyquist plots of the tube cell at potentials indicated in the figure.

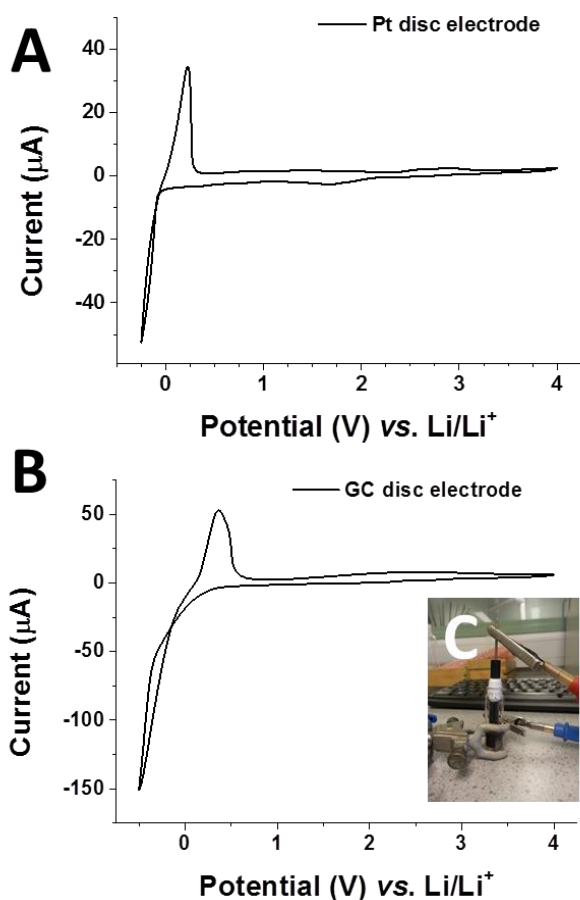


1 Both CVs and AC impedance results in Fig. 2 indicate that the Kuraray Act-C doesn't show  
2 a pure EDLC performance in EMIM[B(CN)<sub>4</sub>]. The Act-C can store more charge in a potential  
3 range from -1.7 to 0 V vs. Ag/Ag<sup>+</sup> than the range of 0 to 1.0 V vs. Ag/Ag<sup>+</sup>. If a symmetrical  
4 supercapacitor was fabricated using this Act-C and ionic liquid, the maximum voltage could not  
5 go beyond 2.7 V. The calculated specific capacitance value of Kuraray Act-C in EMIM[B(CN)<sub>4</sub>]  
6 is about 100 F g<sup>-1</sup>, which is comparable to the value of the same sample got in aqueous  
7 solution.<sup>21</sup> The voltage of this ionic liquid based symmetrical cell is not increased dramatically,  
8 while the resistance of the cell will increased compared to the cell using an aqueous electrolyte.  
9 In this case, changing electrolyte from an aqueous to a non-aqueous electrolyte is not economic.  
10 A new strategy should be made to improve the energy capacity of the cell.

11 As aforementioned, the lithium battery or Li-ion battery processes very high energy capacity  
12 mainly caused by the very negative potential of Li/Li<sup>+</sup> or relevant redox couple. We chose an  
13 ionic liquid which was used as Li-ion battery electrolyte in the following work. The ionic liquid  
14 solution containing LiClO<sub>4</sub> was used as the electrolyte of the supercapattery. The lithium salt is  
15 the Li-ion source for the electrochemical deposition and dissolution of lithium metal on the  
16 negative electrode of the supercapattery.

17 Fig. 3A and 3B shows clearly the electrochemical deposition and dissolution of lithium in  
18 the ionic liquid electrolyte containing lithium salt on a 2 mm diameter Pt disc electrode and a 3  
19 mm diameter Glass Carbon (GC) disc electrode, respectively. Fig 2C is the photo of the  
20 homemade electrochemical cell, in which a working electrode (Pt or GC) and a piece of lithium  
21 metal foil as both counter and reference electrodes are sealed in a vial. The electrolyte contains  
22 0.01 mol L<sup>-1</sup> LiClO<sub>4</sub> in the mixture of BMPyrrFAP and  $\gamma$ -GBL (volume ratio 1:1). Lithium metal  
23 can be electrochemically deposited on both substrate materials, and the fresh deposited lithium is

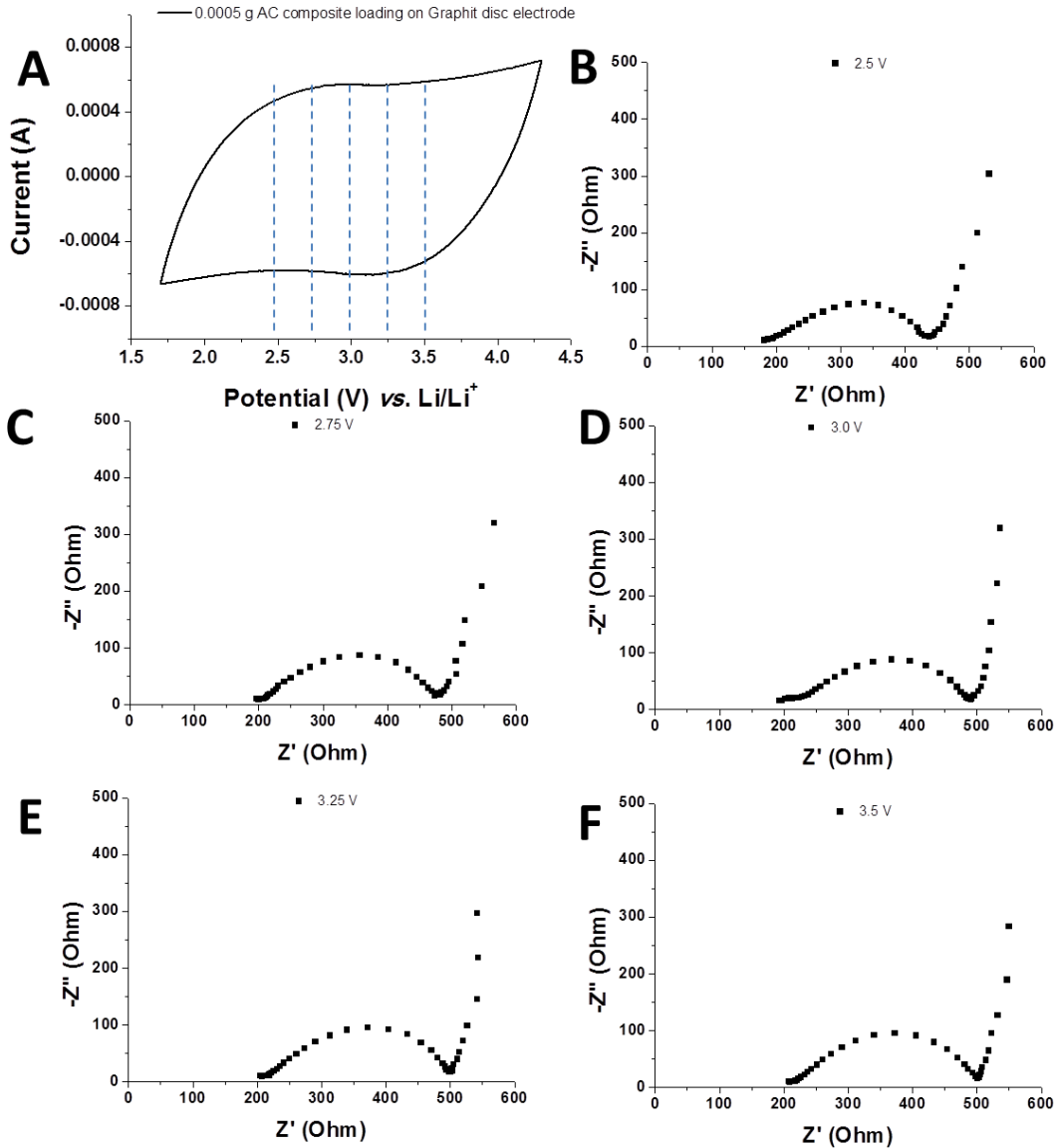
1 stable in the electrolyte unless a positive scan occurs showing a dissolution peak in the CVs. The  
2 over-potential on the GC electrode indicates an energy gap between condensed carbon and lithium  
3 surface. Another key **information** from Fig. 3 is that the ionic liquid solution used in this work  
4 shows an electrochemical window more than 4 V using Pt and GC electrodes. The ionic liquid  
5 solution could be a potential candidate for the supercapattery electrolyte.



6  
7 **Fig. 3** CVs collected on (A) a 2 mm diameter Pt disc electrode and (B) a 3 mm diameter Glass  
8 Carbon disc electrode, in the mixture of BMPyrrFAP and  $\gamma$ -GBL (v:v = 1:1), contains 0.01 mol  
9  $\text{L}^{-1}$   $\text{LiClO}_4$ . Scan rate  $10 \text{ mV s}^{-1}$ . Potential range:  $-0.25 \sim 4.00 \text{ V vs. Li/Li}^+$ . (C) Photo of the  
10 homemade electrochemical cell.

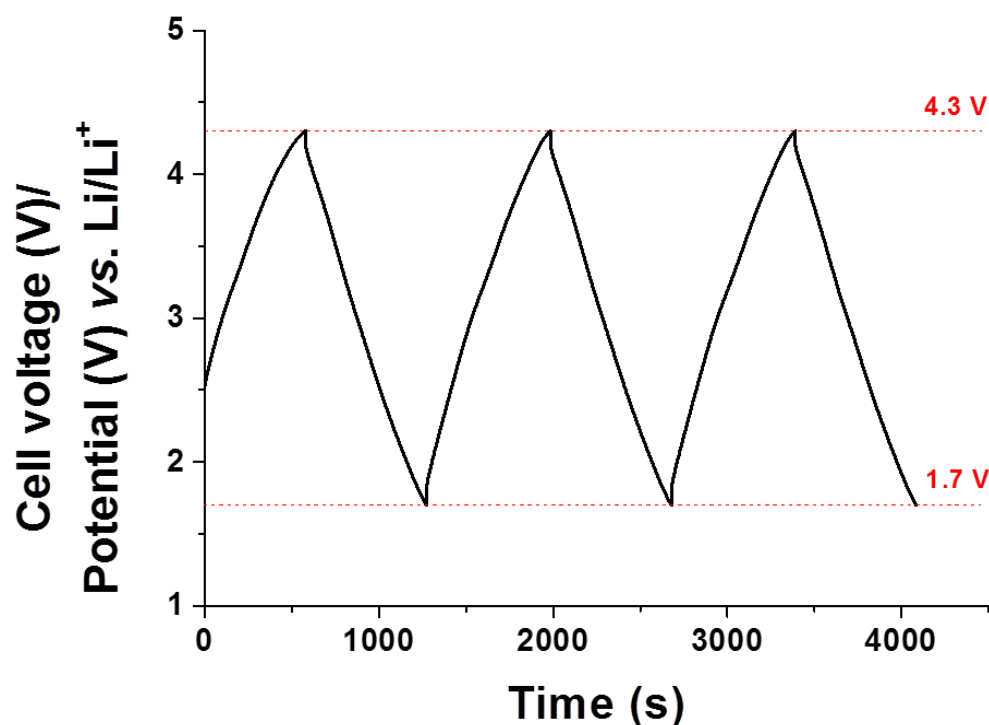
1 In a demonstrative supercapattery cell with lithium metal negative electrode, the redox  
2  $\text{Li}/\text{Li}^+$  reaction should be occurring during the charging or discharging process. A  $0.5 \text{ mol L}^{-1}$   
3  $\text{LiClO}_4$  ionic liquid solution was prepared as the electrolyte to provide sufficient Li-ion in the  
4 electrolyte. The solvent content is the same as the one in the previous lithium deposition  
5 experiment, BMPyrrFAP and  $\gamma$ -GBL (v:v = 1:1). The working electrode is a piece of 0.5 mg  
6 Kuraray Act-C pellet coated on a 5 mm diameter graphite disc electrode with PVDF binder. The  
7 counter and referenced electrodes are lithium metal foil. The cell was fabricated in an argon  
8 filled glove box, sealed properly and then transferred outside the box for the further test. The CV  
9 and AC impedance data of this cell is presented in Fig. 4. The blue dash lines on CV curve mark  
10 the potential at which the AC impedance test was run. It should be mentioned again that the real  
11 amount of lithium metal anticipating the charge storage process is negligible according the  
12 previous calculation. The reason of placing a piece of lithium metal foil in the cell is to acquire  
13 accurate potential result during the charging and discharging processes. From the CV in Fig. 4,  
14 we found that the Kuraray Act-C can undergo a capacitor-like behaviour from the potential range  
15 from 1.7 to 4.3 V vs.  $\text{Li}/\text{Li}^+$  at least. There is no obvious turning point to the clear oxidative or  
16 reductive current on the CV curve. If we assumed this is capacitor behaviour, the calculated  
17 specific capacitance value is  $101 \text{ F g}^{-1}$ . The deformed rectangular CV shape should be caused by  
18 the resistance of the whole cell, which is clearly shown in the Nyquist plots of the cell at  
19 different potentials. Although the resistance of the cell shows a value about  $180 \Omega$ , the  
20 equivalent series resistance (ESR) is about  $35 \Omega \text{ cm}^2$  (area:  $0.196 \text{ cm}^2$ ), which is only 30 times  
21 larger than the value got from a symmetrical aqueous AC supercapacitor using the same  
22 electrode fabricating method.<sup>21</sup> In this case, the resistance as shown in Fig. 4 still falls in the

- 1 acceptable range in practical devices. The optimization of this hybrid design is definitely needed
- 2 to **increase output power**.



- 3
- 4 **Fig. 4** (A) CV of 0.5 mg Kuraray **Act-C** composite (containing 5 % w. PVDF) on a 5 mm
- 5 diameter Graphite disc electrode in mixture of BMPyrrFAP and  $\gamma$ -GBL (v/v = 1/1) containing
- 6  $0.5 \text{ mol L}^{-1} \text{ LiClO}_4$ . Scan rate:  $10 \text{ mV s}^{-1}$ . Nyquist plots of the same cell at the potential of (B)
- 7 2.50 V, (C) 2.75 V, (D) 3.00 V, (E) 3.25 V, (F) 3.50 V vs Li/Li<sup>+</sup>. A Lithium foil was used as the
- 8 reference and counter electrodes. Frequent range: 10 kHz ~ 0.01 Hz.

1



2

3 **Fig. 5** Galvanostatic charge-discharge curves of a pellet of 0.5 mg Kuraray **Act-C** composite  
4 (containing 5 % w. PVDF) on a 5 mm diameter graphite disc electrode in mixture of  
5 BMPyrrFAP and  $\gamma$ -GBL (v/v = 1/1) containing  $0.5 \text{ mol L}^{-1} \text{ LiClO}_4$ . Current density:  $1 \text{ mA cm}^{-2}$ .

6

7 The galvanostatic charge-discharge test was run under a current density of  $1.02 \text{ mA cm}^{-2}$ .  
8 Because the negative electrode is a lithium foil, the voltage of the cell decays smoothly and  
9 linearly during the discharging process from 4.3 to 1.7 V. **Because** the charging and discharging  
10 curve is almost symmetric, we still can calculate the specific capacitance and energy capacity by  
11 the method for supercapacitor. The **Act-C** specific capacitance value comes to  $107 \text{ F g}^{-1}$  in the  
12 ionic liquid solution containing  $\text{LiClO}_4$ . Noted that only tiny amount of lithium metal takes part  
13 in the charge transfer during the charging and discharging process and the molecular weight of

1 Lithium is only  $6.94 \text{ g mol}^{-1}$ , we can ignore the mass of the negative electrode if the active  
2 materials are counted only in the calculation of specific energy capacity. The value is  $232 \text{ Wh}$   
3  $\text{kg}^{-1}$ .

4 If we only chose an ionic liquid as the electrolyte, we can hardly use the available redox  
5 couple resources to store charge in the energy storage devices. The Li-ion source ionic liquids  
6 electrolyte can both supply sufficient charge carrier for the charge storage on the **Act-C** surface  
7 and the necessary Li-ion for the chemical reaction. We do notice that the CV of the **Act-C** in a  
8 pure ionic liquid show partly pseudo-capacitance behaviour. This is a preliminary proof for the  
9 charge transfer or charge isolation process on the carbon surface. The advantage of the organic  
10 electrolytes or ionic liquid electrolytes is that they can keep chemical and thermal stable in a  
11 wider potential or temperature range than the one of aqueous electrolyte. Although recent studies  
12 have revealed that some aqueous electrolyte can be superior to its analogous species on voltage<sup>8</sup>  
13 and temperature limit,<sup>23</sup> the variety and particularity of ionic liquids still make themselves  
14 competitive in different application, especially in energy storage. This paper reveals a new idea  
15 on using the **Act-C** materials as a positive electrode material in supercapattery. The following-up  
16 work on further understanding the charge storage mechanism of **Act-C** in ionic liquids and  
17 optimization of the hybrid design of the supercapattery in this paper is ongoing.

18

## 19 **Conclusions**

20 A hybrid supercapattery design comprising a lithium metal negative electrode and an  
21 activated carbon positive electrode is presented and demonstrated using an experimental cell in  
22 this paper. An ionic liquid was used as one component of the electrolyte containing  $\text{LiClO}_4$ . The  
23 Kuraray activated carbon shows both EDLC and pseudo-capacitor behaviour in a solo ionic

1 liquid electrolyte. In the ionic liquid solution, the sufficient Li-ion in the ionic liquid electrolyte  
2 provide additional charge carriers and enough charge storage species through the Li/Li<sup>+</sup> redox  
3 reaction. The energy capacity of the demonstrative supercapattery reaches to 232 Wh kg<sup>-1</sup>, while  
4 the device can present capacitor-like behaviour when the Galvanostatic charge-discharge current  
5 density is more than 1.0 mA cm<sup>-2</sup>, maintaining its high power output character. In addition, the  
6 partly pseudo-capacitor behaviour of the activated carbon in ionic liquid reveal a possibility to  
7 study the interaction of redox species inside the micropore structure of the activated carbon  
8 materials.

## 10 **Acknowledgements**

11 This work received funding from the University of Nottingham Ningbo China and Ningbo  
12 Municipal Government (3315 Plan and IAMET Special Fund, 2014A35001-1). Responsibility  
13 for the content of this paper lies with the authors.

## 15 **Notes and references**

- 16 1. A. J. Stevenson, D. G. Gromadskyi, D. Hu, J. H. Chae, L. Guan, L. P. Yu and G. Z. Chen, in  
17 *Nanocarbons for Advanced Energy Storage*, Vol. 1, ed. X. Feng, Wiley-VCH, Weinheim,  
18 2015, 179-210.
- 19 2. S. W. Woo, K. Dokko, H. Nakano and K. Kanamura, *Electrochemistry*, 2007, **75**, 635-640.
- 20 3. A. Krause, P. Kossyrev, M. Oljaca, S. Passerini, M. Winter and A. Balducci, *J. Power*  
21 *Sources*, 2011, **196**, 8836-8842.
- 22 4. K. C. Ng, S. W. Zhang, C. Peng and G. Z. Chen, *J. Electrochem. Soc.*, 2009, **156**, A846-  
23 A853.

- 1 5. S. W. Zhang, C. Peng, K. C. Ng and G. Z. Chen, *Electrochim. Acta*, 2010, **55**, 7447-7453.
- 2 6. Z. Dai, C. Peng, J. H. Chae, K. C. Ng and G. Z. Chen, *Sci. Rep.*, 2015, **5**, 09854.
- 3 7. C. Peng, S. Zhang, X. Zhou and G. Z. Chen, *Chem. Comm.*, 2010, **3**, 1499-1502.
- 4 8. J. H. Chae and G. Z. Chen, *Electrochim. Acta*, 2012, **86**, 248-254.
- 5 9. X. Zhou, C. Peng and G. Z. Chen, *AIChE J.*, 2012, **58**, 974-983.
- 6 10. S. Makino, Y. Shinohara, T. Ban, W. Shimizu, K. Takahashi, N. Imanishi and W. Sugimoto,  
7 *RSC Adv.*, 2012, **2**, 12144-12147.
- 8 11. P. Wasserscheid and T. Welton (Eds.), *Ionic Liquids in Synthesis*, Wiley-VCH Verlag  
9 Weinheim/Germany, 2002.
- 10 12. M. Oromi-Farrus, J. Eras, G. Villorbina, M. Torres, V. Llopis-Mestre, T. Welton and R.  
11 Canela, *Anal. Sci.*, 2008, **24**, 1341-1345.
- 12 13. L. Chen, Y. Chi, X. Zheng, Y. Zhang and G. Chen, *Anal. Chem.*, 2009, **81**, 2394-2398.
- 13 14. T. Li, B. Li, S. Dong and E. Wang, *Chem. Eur. J.*, 2007, **13**, 8516-8521.
- 14 15. X. J. Wei, L. P. Yu, D. H. Wang, X. B. Jin and G. Z. Chen, *Green Chem.*, 2008, **10**, 296-305.
- 15 16. X. J. Wei, L. P. Yu, X. B. Jin, D. H. Wang and G. Z. Chen, *Adv. Mater.*, 2009, **21**, 776-780.
- 16 17. L. P. Yu and G. Z. Chen, *RSC Adv.*, 2014, **4**, 40281-40285.
- 17 18. M. Anouti, E. Couadou, L. Timperman and H. Galiano, *Electrochim. Acta*, 2012, **64**, 110-  
18 117.
- 19 19. A. Orita, K. Kamijima and M. Yoshida, *J. Power Sources*, 2010, **195**, 7471-7479.
- 20 20. M. Galinski and I. Stepniak, *J. Appl. Electrochem.*, 2009, **39**, 1949-1953.
- 21 21. D. G. Gromadskyi, J. H. Chae, S. A. Norman and G. Z. Chen, *Appl. Energ.*, 2015, **159**, 39-  
22 50.



- 1 22. L. P. Yu, H.J. Sun, J. He, D. H. Wang, X. B. Jin, X. H. Hu and G.Z. Chen, *Electrochem.*
- 2 *Commun.*, 2007, **9**, 1374-1381.
- 3 23. Y. Gao, Z. Qin, L. Guan, X. Wang and G. Z. Chen, *Chem. Commun.*, 2015, **51**, 10819-
- 4 10822.
- 5